

THE ELECTROMAGNETIC COUNTERPART OF THE BINARY NEUTRON STAR MERGER LIGO/VIRGO GW170817: VIII. A COMPARISON TO COSMOLOGICAL SHORT-DURATION GAMMA-RAY BURSTS

W. FONG,^{1,*} E. BERGER,² P. K. BLANCHARD,² R. MARGUTTI,¹ P. S. COWPERTHWAIT,² R. CHORNOCK,³ K. D. ALEXANDER,²
B. D. METZGER,⁴ V. A. VILLAR,² M. NICHOLL,² T. EFTEKHARI,² P. K. G. WILLIAMS,² J. ANNIS,⁵ D. BROUT,⁶ D. A. BROWN,⁷
H.-Y. CHEN,⁸ Z. DOCTOR,⁸ H. T. DIEHL,⁵ D. E. HOLZ,^{9,8} A. REST,^{10,11} M. SAKO,⁶ AND M. SOARES-SANTOS^{5,12}

¹*Center for Interdisciplinary Exploration and Research in Astrophysics (CIERA) and Department of Physics and Astronomy, Northwestern University, Evanston, IL 60208*

²*Harvard-Smithsonian Center for Astrophysics, 60 Garden Street, Cambridge, Massachusetts 02138, USA*

³*Astrophysical Institute, Department of Physics and Astronomy, 251B Clippinger Lab, Ohio University, Athens, OH 45701, USA*

⁴*Department of Physics and Columbia Astrophysics Laboratory, Columbia University, New York, NY 10027, USA*

⁵*Fermi National Accelerator Laboratory, P.O. Box 500, Batavia, IL 60510, USA*

⁶*Department of Physics and Astronomy, University of Pennsylvania, Philadelphia, PA 19104, USA*

⁷*Department of Physics, Syracuse University, Syracuse NY 13224, USA*

⁸*Kavli Institute for Cosmological Physics, University of Chicago, Chicago, IL 60637, USA*

⁹*Enrico Fermi Institute, Department of Physics, Department of Astronomy and Astrophysics*

¹⁰*Space Telescope Science Institute, 3700 San Martin Drive, Baltimore, MD 21218, USA*

¹¹*Department of Physics and Astronomy, The Johns Hopkins University, 3400 North Charles Street, Baltimore, MD 21218, USA*

¹²*Department of Physics, Brandeis University, Waltham, MA 02452, USA*

ABSTRACT

We present a comprehensive comparison of the properties of the radio through X-ray counterpart of GW170817 and the properties of short-duration gamma-ray bursts (GRBs). For this effort, we utilize a sample of 36 short GRBs spanning a redshift range of $z \approx 0.12 - 2.6$ discovered over 2004-2017. We find that the counterpart to GW170817 has an isotropic-equivalent luminosity that is ≈ 3000 times less than the median value of on-axis short GRB X-ray afterglows, and $\gtrsim 10^4$ times less than that for detected short GRB radio afterglows. Moreover, the allowed jet energies and particle densities inferred from the radio and X-ray counterparts to GW170817 and on-axis short GRB afterglows are remarkably similar, suggesting that viewing angle effects are the dominant, and perhaps only, difference in their observed radio and X-ray behavior. From comparison to previous claimed kilonovae following short GRBs, we find that the optical and near-IR counterpart to GW170817 is comparatively under-luminous by a factor of $\approx 3 - 5$, indicating a range of kilonova luminosities and timescales. A comparison of the optical limits following short GRBs on $\lesssim 1$ day timescales also rules out a “blue” kilonova of comparable optical isotropic-equivalent luminosity in one previous short GRB. Finally, we investigate the host galaxy of GW170817, NGC 4993, in the context of short GRB host galaxy stellar population properties. We find that NGC 4993 is superlative in terms of its large luminosity, old stellar population age, and low star formation rate compared to previous short GRB hosts. Additional events within the Advanced LIGO/Virgo volume will be crucial in delineating the properties of the host galaxies of NS-NS mergers, and connecting them to their cosmological counterparts.

* Hubble Fellow

1. INTRODUCTION

Short-duration gamma-ray bursts (GRBs) have long been linked to compact object merger progenitors (Eichler et al. 1989; Narayan et al. 1992), involving two neutron stars (NS-NS) or a neutron star and a black hole (NS-BH). This link has been strengthened by a wealth of indirect observational evidence: the lack of associated supernovae to deep optical limits (Fox et al. 2005; Hjorth et al. 2005a,b; Soderberg et al. 2006; Kocevski et al. 2010; Rowlinson et al. 2010; Berger 2014; Fong et al. 2014), the observed optical/near-IR excess emission following some short GRBs interpreted as r -process kilonovae (Perley et al. 2009; Berger et al. 2013; Tanvir et al. 2013; Jin et al. 2015; Yang et al. 2015; Jin et al. 2016), the locations of short GRBs within their host galaxies which are well-matched to predictions for NS-NS mergers (Fong et al. 2010; Fong & Berger 2013), and the sizable fraction of short GRBs that occur in early-type galaxies (Berger et al. 2005; Gehrels et al. 2005; Bloom et al. 2006; Fong et al. 2013), indicative of older stellar progenitors (Zheng & Ramirez-Ruiz 2007). While this indirect evidence has been strongly in favor of NS-NS/NS-BH merger progenitors, to date there has been no direct evidence linking short GRBs to their origin.

The Advanced Laser Interferometer Gravitational-Wave Observatory (LIGO) and Advanced Virgo announced the detection of a gravitational wave candidate on 2017 August 17 at 12:41:04 UT with a high probability of being a NS-NS merger (LIGO Scientific Collaboration and Virgo Collaboration 2017b,a). At 12:41:06.47 UT, a weak, gamma-ray transient with a duration of ~ 2 sec was discovered by the Gamma-ray Burst Monitor (GBM) on-board the *Fermi* satellite (Goldstein et al. 2017), with a delay of ≈ 2 s from the aLIGO/Virgo trigger time. The near-coincident detection of a gamma-ray transient and a neutron star merger detected by gravitational waves potentially provides the first “smoking gun” evidence that at least some short GRBs originate from neutron star mergers.

Following the detection, our search with the Dark Energy Camera (DECam) yielded the detection of an optical transient located at RA=13^h 09^m 48.08^s and Dec=−23°22′53.2″ (J2000; Soares-Santos et al. 2017), situated $\sim 10''$ from NGC 4993 (Helou et al. 1991). This fading optical transient¹ was demonstrated to be the likely optical counterpart to GW170817 from its temporal evolution (Cowperthwaite et al. 2017). We initiated observations across the electromagnetic spectrum, and discovered a brightening X-ray source (Margutti et al. 2017), monitored the evolution of the transient with optical (Nicholl et al. 2017) and near-IR spec-

troscopy (Chornock et al. 2017), and detected the radio counterpart at GHz frequencies (Alexander et al. 2017). The details and interpretation of each data set are described in the individual papers.

Here, we leverage our extensive data set of the electromagnetic counterpart to GW170817 to provide a broader picture of the event in the context of the cosmological short GRB population. In particular, we examine the counterpart with respect to short GRB afterglows, searches for kilonovae following short GRBs, and short GRB locations with respect to their host galaxies. We also examine the host galaxy NGC 4993 with respect to the stellar population properties of galaxies hosting short GRBs.

Unless otherwise noted, all magnitudes in this paper are in the AB system and reported uncertainties correspond to 68% confidence. We employ a standard Λ CDM cosmology with $\Omega_M = 0.27$, $\Omega_\Lambda = 0.73$, and $H_0 = 71.0 \text{ km s}^{-1} \text{ Mpc}^{-1}$. We note that all luminosities quoted in this paper correspond to isotropic-equivalent values. We adopt a distance to both NGC 4993 and the counterpart of $D_L = 39.5 \text{ Mpc}$ (Helou et al. 1991).

2. SAMPLE & OBSERVATIONS

We collect observations of previous, well-localized short GRBs across the electromagnetic spectrum, as well as observations of their host galaxies.

2.1. Redshifts

To enable an effective comparison to the counterpart to GW170817, we utilize data from all previous short GRBs with redshift measurements. We compile redshift measurements from Berger (2014) for bursts discovered over 2004–2013. To update this sample, we also include redshifts for new bursts from GCN circulars (Hartoog et al. 2014; Cucchiara & Levan 2016; Levan et al. 2016), recent papers on individual events (Fong et al. 2016; Troja et al. 2016; Selsing et al. 2017), and additional optical spectroscopy which will be described in an upcoming work (Fong et al. in prep). Our total sample of short GRBs with redshifts comprises 36 events and spans a redshift range of $\approx 0.12 - 2.6$, with a median of $\langle z \rangle \approx 0.46$ (Figure 1).

We note that, by default, requiring that the events have redshifts only includes bursts that are well-localized to \lesssim few arcsec uncertainty via the detection of an X-ray afterglow. However, we previously explored any potential bias within the *Swift* short GRB population introduced by requiring an X-ray afterglow based on a smaller sample of events (Fong et al. 2013). We found that the large majority of bursts that did not have detected X-ray afterglows were affected by observing constraints that would generally be decoupled from any burst or host galaxy properties. Thus, we do not expect the re-

¹ This source is also known as AT2017gfo (International Astronomical Union name), SSS17a (Coulter et al. 2017b,a), and DLT17ck (Yang et al. 2017; Valenti et al. 2017).

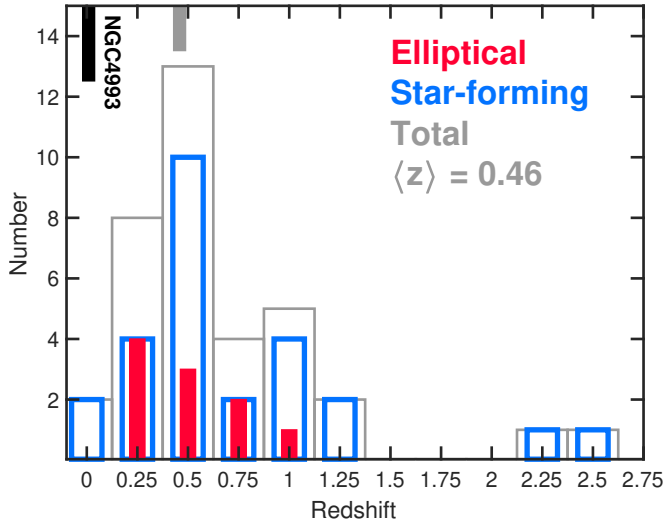


Figure 1. Redshift distribution of 36 short GRBs discovered over 2004-2017 (grey). The distributions are divided by host galaxy type: elliptical (red) and star-forming (blue) galaxies. The redshift of NGC4993 is denoted (black line), along with the median for the short GRB population (grey line) of $\langle z \rangle \approx 0.46$.

quirement of a redshift to introduce any discernible bias in this sample.

2.2. X-rays

In order to compare the X-ray emission of on-axis short GRB afterglows to the X-ray counterpart for GW170817 (Evans et al. 2017; Margutti et al. 2017), we utilize the sample in Fong et al. (2015) which covers short GRBs discovered between November 2004 and March 2015 (references for individual data sets therein). The data were taken primarily with the X-ray Telescope (XRT; Burrows et al. 2005) on-board the *Swift* satellite (Gehrels et al. 2004), the *Chandra X-ray Observatory* and *XMM-Newton*. To supplement this data set, we gather all *Swift*/XRT observations from the light curve repository (Evans et al. 2007, 2009) for short GRBs with detected afterglows between March 2015 and August 2017. To enable a direct comparison to the X-ray counterpart to GW170817, we use the burst redshifts to convert to X-ray luminosity. Our sample of short GRBs with X-ray afterglows comprises 36 events, and the light curves are shown in Figure 2.

2.3. Radio

We compile radio observations for short GRBs in a similar manner to that for the X-ray observations, starting with the sample from Fong et al. (2015). We update this sample to include five additional events with observations from the Karl G. Jansky Very Large Array (VLA) under Programs 15A-235 (PI: Berger) and 17A-218 (PI: Fong). Of the bursts with redshifts, four have previously-reported detections (Berger et al. 2005; Soderberg et al. 2006; Fong et al. 2014, 2015) while

two additional detections are included in the updated sample. In total, the sample includes six bursts with detections and 19 additional events with upper limits. We convert the data to luminosity via the burst redshifts. The resulting radio light curves and upper limits, along with the results of radio monitoring following GW170817 at 6 GHz and 10 GHz with the VLA (Alexander et al. 2017), are shown in Figure 2.

2.4. Optical/Near-IR Kilonovae

There have been three previous claims of kilonovae in the literature: a near-IR excess following GRB 130603B ($z = 0.356$; Berger et al. 2013; Tanvir et al. 2013), and optical excesses following GRB 050709 ($z = 0.16$; Jin et al. 2016) and GRB 060614² ($z = 0.125$; Jin et al. 2015; Yang et al. 2015). We note an additional optical excess was reported following GRB 080503 (Perley et al. 2009); however, since this burst does not have a known redshift, we do not include it in this discussion. To enable a comparison of the luminosity and temporal behavior of the optical/near-IR counterpart to GW170817 (Cowperthwaite et al. 2017; Chornock et al. 2017; Nicholl et al. 2017), we collect observations corresponding as close as possible to the rest-frame r - and H -bands for each burst (Berger et al. 2013; Tanvir et al. 2013; Jin et al. 2015, 2016).

We supplement these detections with any optical/near-IR observations following short GRBs on timescales of $\gtrsim 1$ day after the burst. To this end, we retrieve *Hubble Space Telescope* (*HST*) observations (PI: Tanvir; Program 14237) of the short GRB 160821B from the Mikulski Archive for Space Telescopes (MAST) archive. We utilize observations taken with the Wide Field Camera 3 (WFC3) in the F160W filter, corresponding to rest-frame H -band at the redshift of the burst ($z = 0.16$; Levan et al. 2016), on 2016 September 14 UT (~ 23 days after the burst). We used the *astrodizzle* task as part of the Drizzlepac software package (Gonzaga 2012) to create final drizzled image, using `final_scale` = $0.065'' \text{ pixel}^{-1}$ and `final_pixfrac` = 0.8. We use standard tasks in IRAF to perform aperture photometry of faint point sources in the field to calculate a 3σ limit of $m_{160W} \gtrsim 26.0$ mag.

We add to this sample optical and near-IR upper limits following 14 additional events with redshifts. Compared to the sample in Fong et al. (2015), we note the addition of a deep limit following GRB 050509B of $r \gtrsim 25.7$ mag at ≈ 25.9 hr after the burst (Cenko et al. 2005; Bloom et al. 2006). Although this limit corresponds to rest-frame V -band, we note that the expected $V - r$ color based on observations of the op-

² GRB 060614 had a duration of ≈ 108 seconds and would typically be classified as a long-duration GRB. However, this event lacks an associated supernova to deep limits, suggesting that it does not have a massive star progenitor (Gal-Yam et al. 2006), and thus we include it in this discussion.

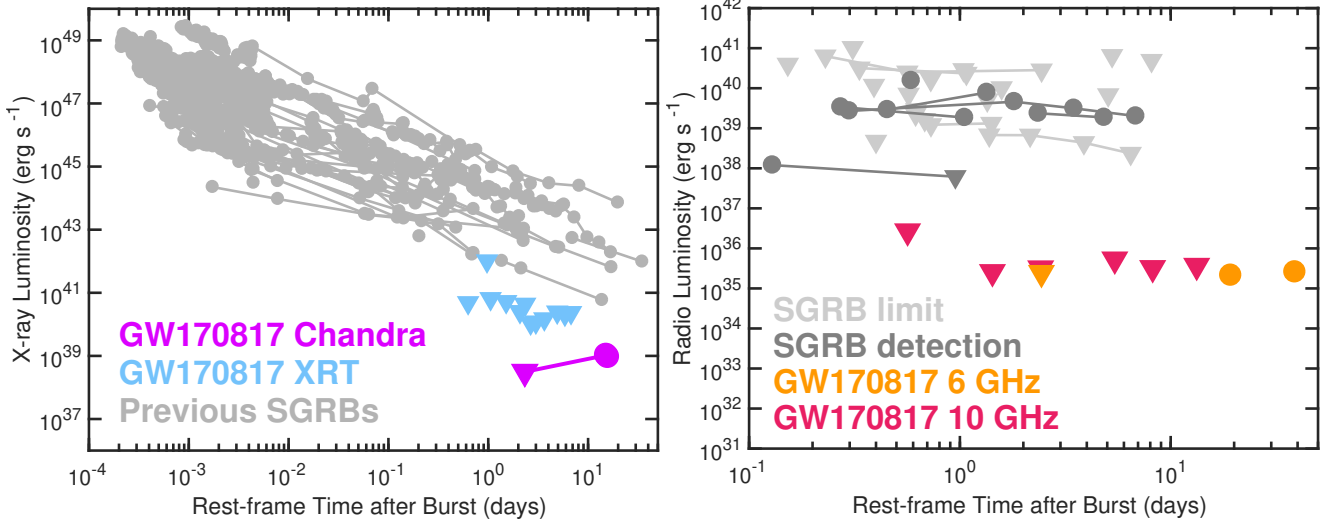


Figure 2. *Left:* Light curve of the X-ray counterpart to GW170817 from *Swift* and *Chandra* (0.3–10 keV; Haggard et al. 2017a,b; Margutti et al. 2017, where circles denote detections and triangles denote 3σ upper limits). Also shown are on-axis X-ray afterglow light curves from all previous short GRBs with well-sampled X-ray light curves and redshifts, comprising 36 events. At the time of detection, GW170817 has an isotropic-equivalent luminosity that is ≈ 3000 times less than the median short GRB X-ray afterglow, and ≈ 50 times less than the faintest detected X-ray emission from a short GRB. *Right:* Radio search for the counterpart of GW170817 from Alexander et al. (2017) at 6 GHz (orange) and 10 GHz (red) with the VLA, yielding detections at 6 GHz beyond ≈ 19 days. The six short GRBs with radio afterglow detections (dark grey circles) along with 3σ upper limits for 19 additional events with redshifts (light grey triangles) are shown. These observations demonstrate that the radio counterpart to GW170817 is $\gtrsim 10^4$ times less luminous (isotropic-equivalent) than detected radio afterglows at similar epochs, and $\gtrsim 500$ times less luminous than the faintest detected radio afterglow for a short GRB.

tical counterpart to GW170817 at ≈ 1.5 days after the event (Cowperthwaite et al. 2017) is negligible, $\lesssim 0.2$ mag. Thus, we still include this point in our sample.

For all bursts with detections of or limits on kilonova emission, we use the burst redshifts to convert apparent magnitude to K -corrected absolute magnitudes. The data for the previous short GRBs, as well as Gemini-South H -band observations of the counterpart to GW170817 (Cowperthwaite et al. 2017) are shown in Figure 3. To enable a direct comparison to early short GRB optical limits, we also employ the initial DECam observation at i -band at ≈ 0.47 days, and correct for the observed $r-i$ color of ≈ 0.2 mag at ≈ 1.4 days (Cowperthwaite et al. 2017). We note that this is conservative as the source has a blue color at $\lesssim 1$ day and 0.2 mag is likely an upper limit on the $r-i$ color.

2.5. Host galaxy properties

To obtain a complete sample of short GRB host properties, we collect all available values for host redshifts, galaxy type, rest-frame B -band luminosity (L_B), stellar mass (M_*), stellar population age (τ), and star formation rate (SFR) from large samples (Leibler & Berger 2010; Fong et al. 2013; Berger 2014) as well as papers on individual objects (Perley et al. 2012; de Ugarte Postigo et al. 2014; Fong et al. 2016; Troja et al. 2016; Selsing et al. 2017). We supplement this sample with values for the redshifts and stellar population properties of eight additional short GRB hosts discovered over 2014–2017, the details of which will be described

in an upcoming work (Fong et al. in prep.). For these bursts, we infer stellar masses from a combination of broad-band SED fitting, and K -band luminosity and $B-K$ color relations (Bell & de Jong 2001; Mannucci et al. 2005). We calculate rest-frame B -band luminosities from host photometry. We normalize these values to the characteristic luminosity (L^*) of the evolving galaxy luminosity function over $z \sim 0$ to $z \approx 2$ depending on the redshift of each host (Blanton et al. 2003; Willmer et al. 2006; Marchesini et al. 2007). The median of each stellar population property is listed in Table 1. The total sample of 36 events provides a comprehensive comparison sample for NGC 4993.

3. COMPARISON TO SHORT GRBS

3.1. Afterglows & Explosion Properties

We first compare the radio and X-ray observations of the counterpart to GW170817 to those following on-axis short GRBs. In the X-ray band, the counterpart is observed to brighten over ≈ 2.4 –15.4 days, indicative of a weak on-axis jet or an off-axis afterglow observed at an angle θ_{obs} from the jet axis (Margutti et al. 2017). At the time of the first detection reported in Margutti et al. (2017) at ≈ 15.4 days, the X-ray counterpart has a luminosity of $\approx 1.1 \times 10^{39}$ erg s $^{-1}$ (0.3–10 keV). The median luminosity of the five short GRBs that have X-ray detections at similar rest-frame times is $\approx 3 \times 10^{42}$ erg s $^{-1}$ (Figure 2); thus, the X-ray counterpart to GW170817 is ≈ 3000 times less luminous. Moreover,

the X-ray counterpart to GW170817 is ≈ 50 times less luminous than the faintest known X-ray emission from a short GRB. Given that the depths of late-time observations following short GRBs are essentially at the limits of current X-ray observatories, Figure 2 demonstrates that the counterpart to GW170817, if shifted to the redshifts of short GRBs, would not have been detected.

The radio afterglows of short GRBs provide a complementary comparison sample. Alexander et al. (2017) report monitoring of the radio counterpart to GW170817 spanning ≈ 0.6 –40 days, with deep limits of $\gtrsim (2-5) \times 10^{35} \text{ erg s}^{-1}$ until ≈ 19 days and detections of $\approx (2.1-2.6) \times 10^{35} \text{ erg s}^{-1}$ thereafter (Figure 2). Overall, the radio counterpart to GW170817 is a factor of $\gtrsim 10^4$ times fainter than detected radio afterglows, which have a median of $\approx 4 \times 10^{39} \text{ erg s}^{-1}$. The faintest reported detection of an on-axis radio afterglow was following one of the most nearby known short GRBs, GRB 160821B ($z = 0.16$), with $\approx 1.2 \times 10^{38} \text{ erg s}^{-1}$ (Figure 2), ≈ 500 times more luminous than the radio counterpart to GW170817, and on very different timescales. Based on the radio monitoring by Alexander et al. (2017), the radio counterpart to GW170817 at the distance of even the most nearby known short GRBs would not have been detected.

Margutti et al. (2017) and Alexander et al. (2017) demonstrate that the temporal behavior of the X-ray and radio counterparts can be jointly explained by an off-axis jet. In particular, they find that for a jet opening angle of 15° , set to the median for short GRBs (Fong et al. 2015), the best-fit family of solutions has a range of circumburst densities, $\approx 10^{-4}$ – 0.01 cm^{-3} , jet energies of 10^{49} – 10^{50} erg , and observer angles, $\theta_{\text{obs}} \approx 20$ – 40° , where the range of solutions is dominated by the uncertainty in the microphysical parameters (Alexander et al. 2017; Margutti et al. 2017). The range of allowed energies and densities inferred from the radio and X-ray counterparts to GW170817 is fully consistent with those inferred from on-axis short GRB afterglows, which have medians of $\approx 8 \times 10^{49} \text{ erg}$ and $\approx (0.3-1.5) \times 10^{-2} \text{ cm}^{-3}$, respectively (Fong et al. 2015). This remarkable similarity hints that viewing angle effects are the dominant, and possibly the only, factor causing the difference in the observed radio and X-ray behavior between this event and on-axis short GRBs.

3.2. Optical and Near-IR Kilonovae

Next we compare the luminosity and temporal evolution of the optical/near-IR counterpart to GW170817 (Soares-Santos et al. 2017; Cowperthwaite et al. 2017; Chornock et al. 2017; Nicholl et al. 2017) to previous claims of kilonovae from short GRBs (Figure 3). We also investigate whether previous searches following short GRBs were sensitive enough to detect excess emission with similar luminosities to the counterpart to GW170817.

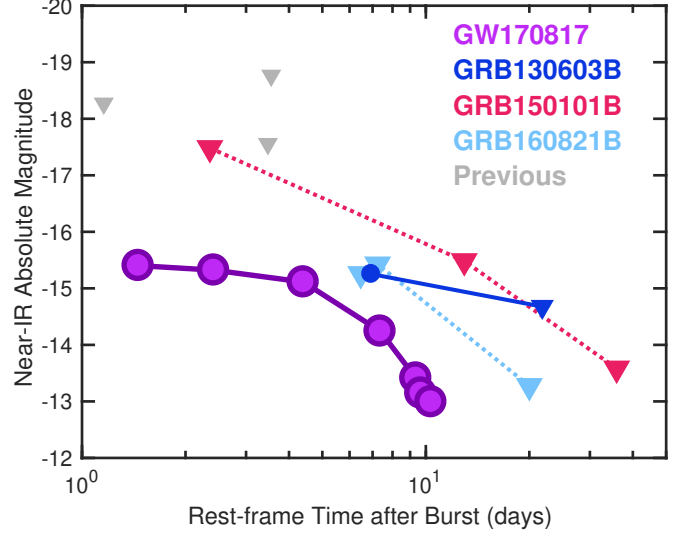


Figure 3. A comparison of the luminosity and temporal evolution of the counterpart to GW170817 to previous claimed kilonovae and late-time searches following short GRBs. The rest-frame near-IR H -band light curves from Gemini-South observations of the counterpart to GW170817 are shown (Cowperthwaite et al. 2017). Also shown is the near-IR excess following GRB 130603B, interpreted as a kilonova (circles; Berger et al. 2013; Tanvir et al. 2013), and 3σ upper limits following previous short GRBs (triangles; Fong et al. 2015, 2016; Kasliwal et al. 2017, and this work). This comparison demonstrates that the near-IR excess following GRB 130603B was ≈ 3 times more luminous than the counterpart to GW170817 at a similar rest-frame time. This also demonstrates that near-IR searches following short GRBs were not sensitive enough or did not occur on the proper timescales to detect a kilonova with similar near-IR luminosity to that of GW170817.

In the rest-frame optical band, the two claimed detections of kilonovae, GRB 050709 (Jin et al. 2016) and GRB 060614 (Yang et al. 2015; Jin et al. 2015), are $\gtrsim 3$ –5 times more luminous than the counterpart to GW170817 at $\gtrsim 3$ days. At near-IR wavelengths, the single detection following GRB 130603B at ≈ 7 days had a luminosity ≈ 30 times greater than the expected level of the afterglow at that time (Berger et al. 2013; Tanvir et al. 2013). This significant near-IR excess, in conjunction with the extremely red color, represents the most convincing case of a kilonova following a cosmological short GRB. The comparison in Figure 3 demonstrates that the near-IR excess following GRB 130603B was substantially more luminous, ≈ 3 times brighter, than the near-IR counterpart to GW170817 at the same epoch (Figure 3). Moreover, all three claimed kilonovae remain luminous for longer after the merger in their respective rest-frame bands.

At the most basic level, the larger observed luminosities and sustained brightness for the three short GRBs could be explained by differences in the masses and velocities of ejected material during and subsequent to the mergers

Table 1. Comparison of Stellar Population Properties

Property	SGRB SF median	SGRB Ell. median	SGRB total median	NGC 4993
(1)	(2)	(3)	(4)	(5)
Stellar Mass ($\log(M_*/M_\odot)$)	9.65 (0.90)	10.85 (0.33)	10.10 (0.72)	10.65
Rest-frame <i>B</i> -band Luminosity (L_B/L_*)	0.70 (1.00)	1.0 (0.80)	0.85 (0.94)	4.2
Star Formation Rate ($M_\odot \text{ yr}^{-1}$)	1.1 (0)	$\lesssim 0.2$ (0)	$\lesssim 0.5$ (0)	0.01
Stellar Population Age (Gyr)	0.26 (1.00)	1.3 (1.00)	0.50 (1.00)	11.2
Projected Physical Offset δR (kpc)	5.5 (0.27)	20.7 (0.17)	6.9 (0.24)	2.1
Fractional Flux	0.14 (0.75)	0.21 (0.80)	0.19 (0.76)	0.54

NOTE—Columns correspond to: (1) Stellar population property, (2) Median for star-forming short GRB hosts, (3) Median for elliptical short GRB hosts, (4) Median for total short GRB host population, and (5) Value for NGC 4993 from [Blanchard et al. \(2017\)](#). In each column, numbers in parentheses represent the fraction of events in each class with values below that of NGC 4993.

(e.g., [Metzger et al. 2010](#); [Barnes & Kasen 2013](#)). For both GRB 050709 and GRB 060614, the inferred ejecta masses and velocities are $\approx 0.05 - 0.1 M_\odot$ and $0.1 - 0.2c$ ([Yang et al. 2015](#); [Jin et al. 2016](#)). Using single-component models available at the time ([Barnes & Kasen 2013](#)), the luminosity of the kilonova following GRB 130603B translated to an ejecta mass of $\approx 0.03 - 0.08 M_\odot$ for velocities of $0.1 - 0.3c$ ([Berger et al. 2013](#)).

However, it has been suggested that there may be an additional early “blue” kilonova component as the result of lanthanide-free material from disk winds, amplified by the formation of hypermassive neutron star following the merger that is at least temporarily stable to collapse ([Metzger & Fernández 2014](#); [Kasen et al. 2015](#); [Metzger 2017](#)). Indeed, observations of the counterpart to GW170817 have demonstrated that single-component models are likely inadequate to explain kilonova behavior. The combination of multi-band optical/near-IR photometry of the counterpart to GW170817 ([Cowperthwaite et al. 2017](#)), high-cadence UV/optical spectroscopy ([Nicholl et al. 2017](#)), and high-cadence near-IR spectroscopy ([Chornock et al. 2017](#)), show evidence for “blue” and “red” kilonova components, with overall lower inferred ejecta masses when compared to values inferred from short GRBs: $0.01 M_\odot$ and $\approx 0.03 - 0.04 M_\odot$, respectively. Still, the comparison between potential kilonovae following short GRBs and the optical/near-IR counterpart to GW170817 suggests that there may be a broad range of kilonova luminosities, colors, and timescales.

Finally, we utilize optical/near-IR upper limits following short GRBs to explore whether such searches would have been sensitive to the optical/near-IR counterpart to GW170817, had it originated at higher redshifts. There are numerous optical limits following short GRBs at $\lesssim 1$ day

from afterglow searches ([Fong et al. 2015](#)), and the deepest limit is following GRB 050509B, with $M_r \approx -14.3$ at ≈ 0.9 days ([Cenko et al. 2005](#); [Bloom et al. 2006](#)). This is ≈ 1 mag deeper, or ≈ 2.2 times less luminous, than the optical brightness of the counterpart to GW170817 ([Cowperthwaite et al. 2017](#); [Soares-Santos et al. 2017](#)) interpolated to the same rest-frame time. Thus, a “blue” kilonova of similar luminosity to GW170817 can be confidently ruled out for GRB 050509B (see also [Hjorth et al. 2005a](#); [Metzger et al. 2010](#)), which also likely originated from an elliptical host galaxy at a low redshift of $z = 0.225$ ([Gehrels et al. 2005](#); [Bloom et al. 2006](#)). We note that since this event was detected as an on-axis short GRB, it is unlikely that there was significant obscuration of any “blue” component by a “red” kilonova component, which is expected to be more equatorial in geometry ([Metzger & Fernández 2014](#)).

Optical and near-IR searches following all remaining short GRBs were not sensitive enough or did not occur on the proper timescales to detect a kilonova with similar luminosities to that of GW170817. If the luminosity of the counterpart to GW170817 is representative of kilonovae from neutron star mergers, then searches following cosmological short GRBs will only probe the brightest end of the kilonova luminosity function. An added complication to additional kilonova detections is that $\approx 30\%$ of on-axis short GRBs have optical afterglow emission that dominates at early times, with a median of $M_r \approx -18.8$ mag at 10 hr ([Berger 2014](#); [Fong et al. 2015](#)). Thus, if the luminosity of GW170817 is representative of most kilonovae, the most promising route to accurately mapping the luminosity function is via Advanced LIGO/Virgo triggers.

3.3. Location

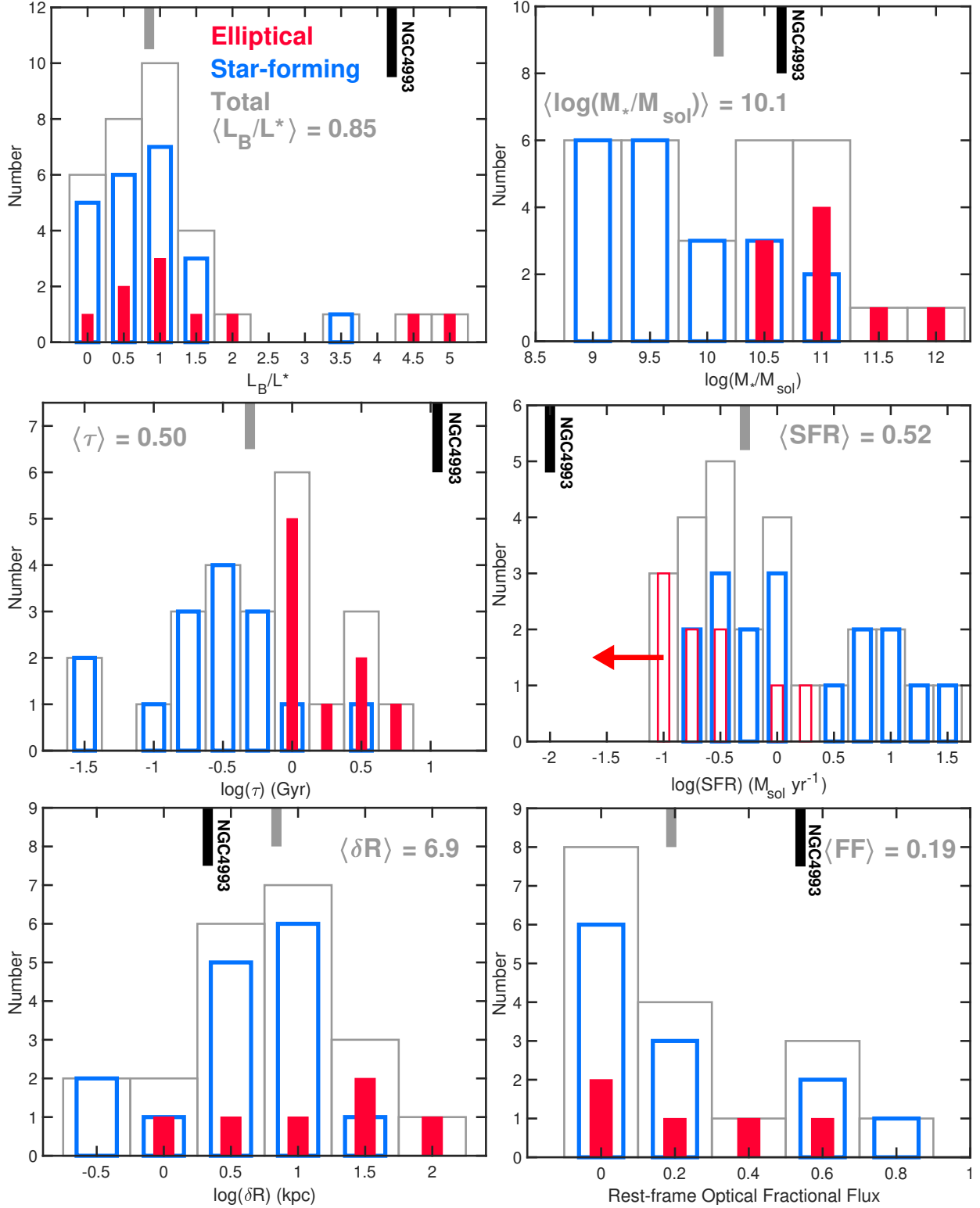


Figure 4. Distributions of stellar population properties for the host galaxies of short GRBs discovered over 2004-2017: rest-frame B -band luminosity (top left), stellar mass (top right), stellar population age (middle left), star formation rate (middle right), projected physical offset (bottom left) and rest-frame optical fractional flux (bottom right). In each panel, the distributions for the total population (grey), star-forming hosts (blue) and elliptical hosts (red) are shown. The location of NGC 4993 in each distribution (black line) along with the median for the short GRB host population (grey line) are marked. For the star formation rate panel, the open red histogram indicates upper limits measured on the star formation rates.

The locations of short GRBs with respect to their host galaxies are an important probe of their progenitor systems, as they contain key information about their local environments at the time of explosion. Past studies have shown that short GRBs have a median projected physical offset (δR) of ≈ 5 kpc (Fong et al. 2010; Fong & Berger 2013), and span a wide range of $\approx 1 - 75$ kpc (Berger 2010; Tunnicliffe et al. 2014). Moreover, as a population, their locations are only very weakly correlated with their underlying host light distributions, indicating that they do not trace the distributions of their hosts’ stellar mass or star formation. In general, their locations demonstrate that the progenitors must migrate from their birth sites to their explosion sites, and have been used as one of the primary arguments that they originate from NS-NS/NS-BH progenitors (Fong et al. 2010; Berger 2010; Fong & Berger 2013; Tunnicliffe et al. 2014).

In this vein, Blanchard et al. (2017) used *HST* optical and near-IR data and found that the counterpart to GW170817 is located at a projected physical offset of ≈ 2.1 kpc from the center of NGC 4993. This value is low compared to short GRBs, with only $\approx 17 - 27\%$ of events located closer to their host centers, regardless of host galaxy type (Figure 4 and Table 1). While the median offset for short GRBs in elliptical hosts is somewhat large, ≈ 21 kpc, this is based on only six events which span the full range of $\approx 1 - 50$ kpc (Figure 4).

A complementary tool to physical offsets is to examine the location of the counterpart to GW170817 with respect to NGC 4993’s light distribution (“fractional flux”). Using this method, Blanchard et al. (2017) found that the counterpart lies on a region of average brightness in the rest-frame optical band, with a fractional flux value of 0.54, indicating that there is nothing unusual about this position with respect to its host stellar mass distribution. However, this value is high compared to short GRBs, with $\approx 75 - 80\%$ of events on lower brightness levels (Figure 4 and Table 1). Together with the small projected physical offset and old stellar population age of ≈ 11.2 Gyr, this implies that the progenitor of GW170817 may have had a comparatively small kick velocity compared to those inferred for short GRBs, or happened to be on a part of its trajectory close to its host at the time of merger. However, since we have no *a priori* information on where the system was born, we can only place an upper limit on the kick velocity using the velocity dispersion of the host galaxy, which Blanchard et al. (2017) find to be $\lesssim 150 - 200$ km s $^{-1}$. Furthermore, if the location of the counterpart to GW170817 is representative, NS-NS mergers may be more correlated to their host stellar mass distribution than implied from short GRBs alone.

3.4. Stellar Population Properties

Characterizing the host galaxy environments of short GRBs is key to understanding the parent stellar popu-

lations in which these explosive transients were born. From fitting the optical and near-IR SED of NGC 4993, Blanchard et al. (2017) found that NGC 4993 has a stellar mass of $\log(M_*/M_\odot) = 10.65$, rest-frame *B*-band luminosity of $\approx 2 \times 10^{10} L_\odot$ ($4.2L^*$ when compared to the local galaxy luminosity function Blanton et al. 2003), stellar population age of ≈ 11.2 Gyr, and star formation rate of $0.01 M_\odot \text{ yr}^{-1}$ (Table 1). Moreover, their analysis from surface brightness profile fitting indicates an elliptical morphology and half-light radius of $\approx 3 - 4$ kpc. Capitalizing on the past decade of short GRB host galaxy studies (Berger 2009; Fong et al. 2013; Berger 2014), we can now compare the stellar population of NGC 4993 with the rest-frame *B*-band luminosities, stellar masses, stellar population ages and star formation rates of short GRB hosts.

The elliptical morphology along with the low level of ongoing star formation in NGC 4993 is consistent with an early-type galaxy designation, which comprise only $\approx 1/3$ of short GRB hosts; the majority of short GRBs occur in star-forming galaxies (Berger 2009; Fong et al. 2013). NGC 4993 is among the most optically luminous host galaxies, superceded only by two other elliptical galaxies at low-redshift: GRB 050509B ($z = 0.225$; Gehrels et al. 2005; Bloom et al. 2006) and GRB 150101B ($z = 0.134$; Fong et al. 2016). However, its half-light radius is at the median level compared to short GRBs of 3.5 kpc, suggesting a comparatively compact morphology.

NGC 4993 also has by far the oldest stellar population age of ≈ 11.2 Gyr, with the short GRBs in our sample spanning $\approx 0.03 - 4.4$ Gyr. Using stellar population age as a proxy for the delay time between the formation and merger of the progenitor system, this suggests a very broad range of delay times, as predicted from population synthesis models of NS-NS binaries (Belczynski et al. 2006). For a delay time distribution of the form $P(\tau) \propto \tau^n$, the stellar population ages of short GRBs, together with the relative burst rates in elliptical and star-forming galaxies, suggest that $n \approx -1$ (Zheng & Ramirez-Ruiz 2007; O’Shaughnessy et al. 2008; Leibler & Berger 2010; Fong et al. 2013). However, if there continues to be an increasing number of detected binary neutron star mergers with long delay times of $\gtrsim 5$ Gyr, the shape of the delay time distribution will shift toward values of $n \gtrsim -1$ (e.g., Zheng & Ramirez-Ruiz 2007). Additional events detected within the Advanced LIGO/Virgo volume will be necessary to provide a low-redshift anchor and delineate the delay time distribution.

In terms of star formation rates, short GRB star-forming hosts span a range of $\approx 0.1 - 30 M_\odot \text{ yr}^{-1}$ (Berger 2009; Perley et al. 2012; Berger et al. 2013; Berger 2014) with a median of $\approx 1.1 M_\odot \text{ yr}^{-1}$, comparable to that of the Milky Way (Table 1). Short GRB hosts with no previous evidence of ongoing star formation had limits of $\lesssim 0.05 - 1.5 M_\odot \text{ yr}^{-1}$

(Berger 2009, 2014; Table 1). In this context, NGC 4993 also has the lowest measured star formation rate of any short GRB host galaxy, enabled by its proximity, and is well below the most constraining limits for cosmological hosts. This low star formation rate is also commensurate with its old stellar population age (Blanchard et al. 2017).

Finally, the inferred stellar masses for the short GRBs in our sample have a median of $\log(M_*/M_\odot) \approx 10.1$ (Table 1). NGC 4993 thus has a comparatively high stellar mass relative to the short GRB population, with $\log(M_*/M_\odot) = 10.65$, as $\approx 70\%$ of hosts have lower stellar masses. Compared to the stellar masses of elliptical galaxies, NGC 4993 is well below average with only $\approx 1/3$ of short GRB elliptical hosts with lower stellar masses.

In summary, NGC 4993 is superlative in its large optical luminosity, old stellar population age, and low star-formation rate compared to the short GRB host population. It is average in terms of its size and above average in terms of its stellar mass.

4. CONCLUSIONS

The past decade of short GRBs serve as a remarkable comparison sample to the counterpart and host galaxy of GW170817. Here, we have provided a thorough comparison between the radio through X-ray counterpart to GW170817 and the afterglows and claimed kilonovae of short GRBs. Additionally, we have placed the host galaxy, NGC 4993, in the context of the galaxies hosting short GRBs. In particular, we conclude the following:

- Compared to on-axis short GRBs, the X-ray counterpart to GW170817 is ≈ 3000 (50) times less luminous than the median (faintest detected) X-ray afterglow luminosity. Similarly, the radio counterpart to GW170817 is $\gtrsim 10^4$ ($\gtrsim 500$) times less luminous than the median (faintest detected) radio afterglows of short GRBs. Shifted to the distances of short GRBs, the counterpart to GW170817 would not have been detected given the capabilities of current X-ray and radio facilities.
- Interpreted as an off-axis jet, the range of allowed energies and densities given by the radio and X-ray modeling (Alexander et al. 2017; Margutti et al. 2017) is strikingly similar to those inferred for short GRBs. This suggests that viewing angle effects are the dominant, and perhaps only, difference between the observed radio and X-ray behavior of this event and on-axis cosmological short GRBs.
- A comparison of the optical and near-IR counterpart to GW170817 to previous claimed kilonovae following short GRBs demonstrates that GW170817 is comparatively under-luminous by a factor of $\approx 3-5$, and

becomes fainter more quickly, suggesting a range of kilonova luminosities and timescales. We further find that a “blue” kilonova of comparable optical luminosity to GW170817 can be ruled out in one previous event, GRB 050509B. In addition, optical and near-IR searches following short GRBs were not sensitive enough or did not occur on the proper timescales to detect a kilonova with similar luminosities to that of GW170817.

- At a projected physical offset of ≈ 2.1 kpc from the center of NGC 4993, the counterpart to GW170817 is relatively close to its host center, with only $\approx 25\%$ of short GRBs more proximal to their hosts. This is consistent with a relatively high fractional flux value, with $\approx 75\%$ of short GRBs on fainter rest-frame optical regions of their host galaxies. This implies that the progenitor of GW170817 may have had a comparatively small kick velocity compared to those inferred for short GRBs, or happened to be on a part of its trajectory close to its host at the time of merger. If the location of the counterpart to GW170817 is representative, NS-NS mergers may be more correlated to their host stellar mass distribution than implied from short GRBs alone.
- In terms of host stellar population properties, NGC 4993 is superlative in terms of its old stellar population age, low star formation rate, and large *B*-band luminosity when compared to the properties of short GRB hosts. NGC 4993 is at the average level for its size and above average for its stellar mass. If the counterpart to GW170817 represents one of a missing population of observable NS-NS mergers with long inferred delay times, additional events within the Advanced LIGO/Virgo volume will be needed to provide a low-redshift anchor and quantify the delay time distribution.

For the first time, we are able to compare the cosmological population of short GRBs to a local analogue. An interesting possibility that arises from the detection of gamma-rays (Goldstein et al. 2017) for an local, off-axis event (as inferred from radio and X-rays; Alexander et al. 2017; Margutti et al. 2017) is that previously-detected, weak short GRBs are in fact local, off-axis events. Indeed, Tanvir et al. (2005) examined a population of BATSE short GRBs that were not well localized and thus did not have redshift determinations, to explore any correlations with local galaxies. They found that up to $\approx 1/4$ of short GRBs may originate at local distances of $\lesssim 100$ Mpc. The fraction of previously-detected weak short GRBs that are actually local, off-axis events will be solidified with additional joint detections of NS-NS/NS-BH mergers from Advanced LIGO/Virgo and gamma-ray transients.

Over the next several years, using the incoming flow of local events from Advanced LIGO/Virgo, we will be able to infer the properties of their jets, delineate the kilonova luminosity distribution, determine the rates of binary neutron star mergers, and infer the properties of their local host galaxies. Such studies will help to define the key similarities, and differences, between the local population of compact object mergers and their cosmological counterparts.

ACKNOWLEDGMENTS

WF acknowledges support for Program number HST-HF2-51390.001-A, provided by NASA through a grant from the Space Telescope Science Institute, which is operated by the

Association of Universities for Research in Astronomy, Incorporated, under NASA contract NAS5-26555. The Berger Time-Domain Group at Harvard is supported in part by the NSF through grants AST-1411763 and AST-1714498, and by NASA through grants NNX15AE50G and NNX16AC22G. DAB is supported by NSF award PHY-1707954. Based on observations made with the NASA/ESA Hubble Space Telescope, obtained from the data archive at the Space Telescope Science Institute. STScI is operated by the Association of Universities for Research in Astronomy, Inc. under NASA contract NAS 5-26555. This work made use of data supplied by the UK Swift Science Data Centre at the University of Leicester. The National Radio Astronomy Observatory is a facility of the National Science Foundation operated under cooperative agreement by Associated Universities, Inc.

REFERENCES

- Alexander et al. 2017, ApJL, Accepted
 Barnes, J., & Kasen, D. 2013, ApJ, 775, 18
 Belczynski, K., Perna, R., Bulik, T., Kalogera, V., Ivanova, N., & Lamb, D. Q. 2006, ApJ, 648, 1110
 Bell, E. F., & de Jong, R. S. 2001, ApJ, 550, 212
 Berger, E. 2009, ApJ, 690, 231
 Berger, E. 2010, ApJ, 722, 1946
 Berger, E. 2014, ARA&A, 52, 43
 Berger, E., Fong, W., & Chornock, R. 2013, ApJL, 774, L23
 Berger, E., et al. 2005, Nature, 438, 988
 Berger, E., et al. 2013, ApJ, 765, 121
 Blanchard et al. 2017, ApJL, Accepted
 Blanton, M. R., et al. 2003, ApJ, 592, 819
 Bloom, J. S., et al. 2006, ApJ, 638, 354
 Burrows, D. N., et al. 2005, SSRv, 120, 165
 Cenko, S. B., Soifer, B. T., Bian, C., Desai, V., Kulkarni, S. R., Schmidt, B. P., Dey, A., & Jannuzi, B. T. 2005, GRB Coordinates Network, 3409
 Chornock et al. 2017, ApJL, Accepted
 Coulter et al. 2017a, Science, Accepted
 Coulter et al. 2017b, GRB Coordinates Network, 21529
 Cowperthwaite et al. 2017, ApJL, Accepted
 Cucchiara, A., & Levan, A. J. 2016, GRB Coordinates Network, 19565
 de Ugarte Postigo, A., et al. 2014, A&A, 563, A62
 Eichler, D., Livio, M., Piran, T., & Schramm, D. N. 1989, Nature, 340, 126
 Evans, P. A., et al. 2009, MNRAS, 397, 1177
 Evans, P. A., et al. 2007, A&A, 469, 379
 Evans et al. 2017, Science, Accepted
 Fong, W., & Berger, E. 2013, ApJ, 776, 18
 Fong, W., et al. 2013, ApJ, 769, 56
 Fong, W., Berger, E., & Fox, D. B. 2010, ApJ, 708, 9
 Fong, W., Berger, E., Margutti, R., & Zauderer, B. A. 2015, ApJ, 815, 102
 Fong, W., et al. 2014, ApJ, 780, 118
 Fong, W., et al. 2016, ApJ, 833, 151
 Fox, D. B., et al. 2005, Nature, 437, 845
 Gal-Yam, A., et al. 2006, Nature, 444, 1053
 Gehrels, N., et al. 2004, ApJ, 611, 1005
 Gehrels, N., et al. 2005, Nature, 437, 851
 Goldstein et al. 2017, ApJL, Accepted
 Gonzaga, S. e. 2012, The DrizzlePac Handbook
 Haggard et al. 2017a, LVC Circulars, 21798
 Haggard et al. 2017b, ApJL, Accepted
 Hartoog, O. E., Malesani, D., Sanchez-Ramirez, R., de Ugarte Postigo, A., Levan, A. J., Fynbo, J. P. U., Vreeswijk, P. M., & Kaper, L. 2014, GRB Coordinates Network, 16437
 Helou, G., Madore, B. F., Schmitz, M., Bica, M. D., Wu, X., & Bennett, J. 1991, in Astrophysics and Space Science Library, Vol. 171, Databases and On-line Data in Astronomy, ed. M. A. Albrecht & D. Egret, 89
 Hjorth, J., et al. 2005a, ApJL, 630, L117
 Hjorth, J., et al. 2005b, Nature, 437, 859
 Jin, Z.-P., et al. 2016, Nature Communications, 7, 12898
 Jin, Z.-P., Li, X., Cano, Z., Covino, S., Fan, Y.-Z., & Wei, D.-M. 2015, ApJL, 811, L22
 Kasen, D., Fernández, R., & Metzger, B. D. 2015, MNRAS, 450, 1777
 Kasliwal, M. M., Korobkin, O., Lau, R. M., Wollaeger, R., & Fryer, C. L. 2017, ApJL, 843, L34
 Kocevski, D., et al. 2010, MNRAS, 404, 963
 Leibler, C. N., & Berger, E. 2010, ApJ, 725, 1202
 Levan, A. J., Wiersema, K., Tanvir, N. R., Malesani, D., Xu, D., & de Ugarte Postigo, A. 2016, GRB Coordinates Network, 19846

- LIGO Scientific Collaboration and Virgo Collaboration. 2017a, Phys. Rev. Lett., Accepted
- LIGO Scientific Collaboration and Virgo Collaboration. 2017b, GRB Coordinates Network, 21509
- Mannucci, F., Della Valle, M., Panagia, N., Cappellaro, E., Cresci, G., Maiolino, R., Petrosian, A., & Turatto, M. 2005, A&A, 433, 807
- Marchesini, D., et al. 2007, ApJ, 656, 42
- Margutti et al. 2017, ApJL, Accepted
- Metzger, B. D. 2017, Living Reviews in Relativity, 20, 3
- Metzger, B. D., & Fernández, R. 2014, MNRAS, 441, 3444
- Metzger, B. D., et al. 2010, MNRAS, 406, 2650
- Narayan, R., Paczynski, B., & Piran, T. 1992, ApJL, 395, L83
- Nicholl et al. 2017, ApJL, Accepted
- O’Shaughnessy, R., Belczynski, K., & Kalogera, V. 2008, ApJ, 675, 566
- Perley, D. A., et al. 2009, ApJ, 696, 1871
- Perley, D. A., Modjaz, M., Morgan, A. N., Cenko, S. B., Bloom, J. S., Butler, N. R., Filippenko, A. V., & Miller, A. A. 2012, ApJ, 758, 122
- Rowlinson, A., et al. 2010, MNRAS, 408, 383
- Selsing, J., et al. 2017, arXiv:1707.01452
- Soares-Santos et al. 2017, ApJL, Accepted
- Soderberg, A. M., et al. 2006, ApJ, 650, 261
- Tanvir, N. R., Chapman, R., Levan, A. J., & Priddey, R. S. 2005, Nature, 438, 991
- Tanvir, N. R., Levan, A. J., Fruchter, A. S., Hjorth, J., Hounsell, R. A., Wiersema, K., & Tunnicliffe, R. L. 2013, Nature, 500, 547
- Troja, E., et al. 2016, ApJ, 827, 102
- Tunnicliffe, R. L., et al. 2014, MNRAS, 437, 1495
- Valenti et al. 2017, ApJL, Accepted
- Willmer, C. N. A., et al. 2006, ApJ, 647, 853
- Yang, B., et al. 2015, Nature Communications, 6, 7323
- Yang et al. 2017, GRB Coordinates Network, 21531
- Zheng, Z., & Ramirez-Ruiz, E. 2007, ApJ, 665, 1220